

1 Supplementary information

2 **Evidence for a consistent use of external cues by marine fish larvae for**
3 **orientation**

4 Igal Berenshtein^{1,2,3}, Robin Faillettaz^{1,4,5}, Jean-Oliver Irisson⁴, Moshe Kiflawi^{6,7}, Ulrike E.
5 Siebeck⁸, Jeffery M. Leis^{9,10}, Claire B. Paris^{1*}

6 ¹*Rosenstiel School of Marine and Atmospheric Science University of Miami 4600 Rickenbacker Causeway, Miami,*
7 *Florida 33149, United-States*

8 ²*Cooperative Institute for Marine and Atmospheric Studies, Rosenstiel School of Marine and Atmospheric*
9 *Science, University of Miami, 4600 Rickenbacker Causeway, Miami, FL 33149, USA*

10 ³*Department of Marine Biology, Leon H. Charney School of Marine Sciences, University of Haifa, Mt. Carmel*
11 *3498838, Haifa, Israel*

12 ⁴*Centre National de la Recherche Scientifique, Laboratoire d'Océanographie de Villefranche-sur-Mer (LOV),*
13 *Sorbonne Universités, UPMC University Paris 06, Villefranche-sur-Mer, France*

14 ⁵*EDECOD (Ecosystem Dynamics and Sustainability), IFREMER, INRAE, Institut Agro, Lorient, France*

15 ⁶*Department of Life-Sciences, Ben-Gurion University of the Negev, POB 653, 84105 Beer-Sheva, Israel*

16 ⁷*The Interuniversity Institute for Marine Sciences of Eilat, Eilat, 88103, Israel*

17 ⁸*Laboratory for Visual Neuroethology, School of Biomedical Sciences, University of Queensland, St Lucia, QLD*
18 *4072, Australia*

19 ⁹*Ecology and Biodiversity Centre, Institute for Marine and Antarctic Studies, University of Tasmania, Hobart, TAS,*
20 *7007, Australia*

21 ¹⁰*Ichthyology, Australian Museum Research Institute, Sydney, NSW, 2001, Australia*

22

23 *Corresponding author: cparis@earth.miami.edu

24 **Supplementary Note 1. Movement analysis of species which do not exhibit higher mean**
25 **vector lengths than expected under CRW**

26 According to the *CRW-vm* simulation analysis, *Chromis atripectoralis*, *C. aureofasciatus* and *A.*
27 *curacao* do not seem to do not exhibit a significantly straighter movement (i.e., higher mean
28 vector length) than expected under CRW, as their *CRW-vm* quantile distribution was not
29 significantly different from the null (i.e., $P > 0.05$, Cohen's $W < 0.25$, Figure S1, Table 1). In
30 contrast, the *CRW-r* analysis of these species indicated that they indeed exhibit a significantly
31 straighter movement than expected under CRW, yet their effect sizes were the lowest among all
32 species (Table 1). Further details regarding the dynamics of *scuba-following* trials¹⁻³ indicate
33 that multiple individuals from *C. aureofasciatus* and *A. curacao* were characterized by
34 distinctive behavior of immediate descent after their release by the observing divers (Figure 2 in
35 ¹ and Figure 6 in ³). This behavior possibly alters the natural orientation behavior observed in the
36 other species (Figure 1), resulting in multiple individuals with \hat{R}_θ values below their expected
37 $R_{\theta^{vm}}$ range (Figure S1). Such pattern can be a result of complex behaviors such as a consistent
38 drift to either right or left, which is manifested as an asymmetrical distribution of *turning angles*
39 ($\Delta\theta$), that is not centered around zero (Figure 1c, Figure S1).

40 For example, the *C. aureofasciatus* larva marked in Figure S1a is characterized by a
41 narrow and asymmetrical distribution of $\Delta\theta$ (Figure S1b), and a nearly uniform distribution of θ
42 (Figure S1c). The dynamics of θ across time (Figure S1c) indicate that the larva consistently
43 made small turns to the left, completing a nearly full circle. Therefore, it is not surprising that \hat{R}_θ
44 is lower than expected under $R_{\theta^{vm}}$, as the larva is essentially swimming in a circle. Similarly, the
45 \hat{R}_θ quantiles of that specific larva is 3% and 1% for the *CRW-r* analysis and the *CRW-vm*
46 analyses respectively, supporting the same conclusion.

47 A further factor for *A. curacao* is that changes in θ between successive measurements ($\Delta\theta$
48) were biased to the left (57.8% left and 42.2% to right), but also differed in the size of the bias
49 and size of $\Delta\theta$ depending on the swimming direction³, i.e., more left than right turns, or made
50 larger left turns, or both. Interestingly, for a larva swimming to the northwest (270° to 360°), left
51 $\Delta\theta$ were 1.67 times more likely, but also the average size of a left $\Delta\theta$ was 6° greater than a right
52 $\Delta\theta$. In contrast, for larvae swimming to the southeast (90° to 180°), a left $\Delta\theta$ was 1.4 more likely
53 than a right $\Delta\theta$, but was only 2° larger. As a result, a larva swimming to the southeast would
54 change direction less over time than a larva swimming in other directions, and those other larvae
55 would be more likely to eventually turn around towards the southeast and southwest.

56

57 **Supplementary Note 2. Wrapped Cauchy as an underlying distribution**

58 Although von Mises distribution is the most commonly used circular distribution for simulating
59 Correlated Random Walk (CRW), other distributions such as wrapped Cauchy were suggested to
60 be more suitable in some cases, for example, when the underlying distribution is a combination
61 of two or more distributions⁴. Based on this we tested the sensitivity of the *CRW-vm* analysis to
62 the underlying type of distribution by replacing the von Mises distribution with a wrapped
63 Cauchy distribution (*CRW-wc*), and accordingly, replacing the *kappa* concentration parameter
64 (n=400, ranging from 0 to 399) with *rho* concentration parameter (n=400, ranging from 0 to
65 0.999). The results indicate that there was no major difference evident between *CRW-vm* and
66 *CRW-wc*, except for the fact that the distribution of quantiles was wider towards the extreme
67 values of $\Delta\theta$ in the x-axis (i.e., $\Delta\theta=0$ and $\Delta\theta=1$). For the *CRW-wc* analysis, same as for *CRW-vm*
68 analysis, the means of all species fall above the $\bar{R}_{\theta^{wc}}$ curve, the confidence intervals of the bulk
69 of species do not overlap with the $\bar{R}_{\theta^{wc}}$ (Figure S2).

70 **Supplementary Note 3. Comparison between scuba-following and DISC experiments for**
71 ***Chromis atripectoralis***

72 Previous studies examined the differences in the orientation patterns of *C. atripectoralis* between
73 *scuba-following* and *DISC* experiments and between individuals and groups of larvae^{5,6}. These
74 studies showed consistency in the findings between the methods, namely in the median
75 swimming directions, the level of directional precision (R_θ). The studies indicated that while
76 both experimental methods indicated that the bulk of larvae swim directionally (Rayleigh's test
77 $p < 0.05$), the *scuba-following* experiments were characterized by higher R_θ values. In addition,
78 the experiments with groups of larvae were characterized by higher R_θ values in both methods.
79 These findings are indeed evident in Figure S3, indicating higher R_θ values for the group
80 experiments in both experimental methods, and higher R_θ values of *scuba-following* compared to
81 the *DISC* experiments. The methodology provided here indicates a higher tendency of the *DISC*
82 experiments for exhibiting a straighter movement than expected under CRW (i.e., higher ΔR_θ
83 and higher quantiles) compared to the *scuba-following*. A sub-sampling of the *DISC* experiments
84 (to $N_{\text{obs}} = 21$) yields comparable results, such that the quantiles of both methods, for individuals
85 and groups, exhibits positive ΔR_θ values, and quantile means that range between the 50th and the
86 85th quantiles, indicating a tendency for exhibiting a straighter movement than expected under
87 CRW (Table 1).

88 The significance of the chi-square tests, however, is not consistent across the different
89 sets of trials. For example, for the *DISC* trials, chi-square tests of *C. atripectoralis* individuals of
90 both *CRW-vm* and *CRW-r* methods, are significant, but for the *C. atripectoralis* groups, *CRW-r*
91 chi-square test is significant and *CRW-vm* is not (Table 1). For the *scuba-following* trials and for
92 the subsampled *DISC* data, chi-square test was significant only for the *CRW-r* method for *C.*
93 *atripectoralis scuba-following* trials. Chi-square test was not significant for *C. atripectoralis*

94 group subsampled *DISC* experiments or for the individual *C. atripectoralis* CRW-vm method of
95 the *scuba-following* trials (Table 1). For the group *scuba-following trials*, there were not
96 sufficient number of trials to conduct the chi-square goodness of fit analysis (Table 1).

97 **Supplementary Note 4. Simulation of irregular unoriented movement patterns.**

98 While our results provide indication for oriented movement by fish larvae, it does not cover all
99 possible behaviors that may be exhibited by moving animals. Complex movement patterns that
100 do not follow the classic definition of CRW, BRW and BCRW are not suitable for our analyses.
101 In this section we simulate six different behaviors under variable number of observations and
102 κ values. Three of these behaviors are the classic patterns of CRW (unoriented), BRW and
103 BCRW (oriented). The other three behaviors represent special patterns that include composite
104 random walk (i.e., κ changes during the trial), “zig zag” movement (i.e., $\Delta\theta$ are drawn from
105 two von-Mises distributions centered around positive and one negative values), and one-sided
106 drift (i.e., $\Delta\theta$ are drawn from a von-Mises distributions that is not centered around zero). While
107 the classic patterns are located in the phase diagram as expected, with CRW on the $R_{\theta_0^{vm}}$ mean
108 curve, BRW located above the 95% $R_{\theta_0^{vm}}$ quantile, and BCRW located in between the two. The
109 special behaviors can be falsely categorized, for example the undirected “zig zag” and the
110 composite CRW behaviors are categorized as indication for directed movement. Details about
111 the simulations and the implemented movement parameters are given in Table S1.

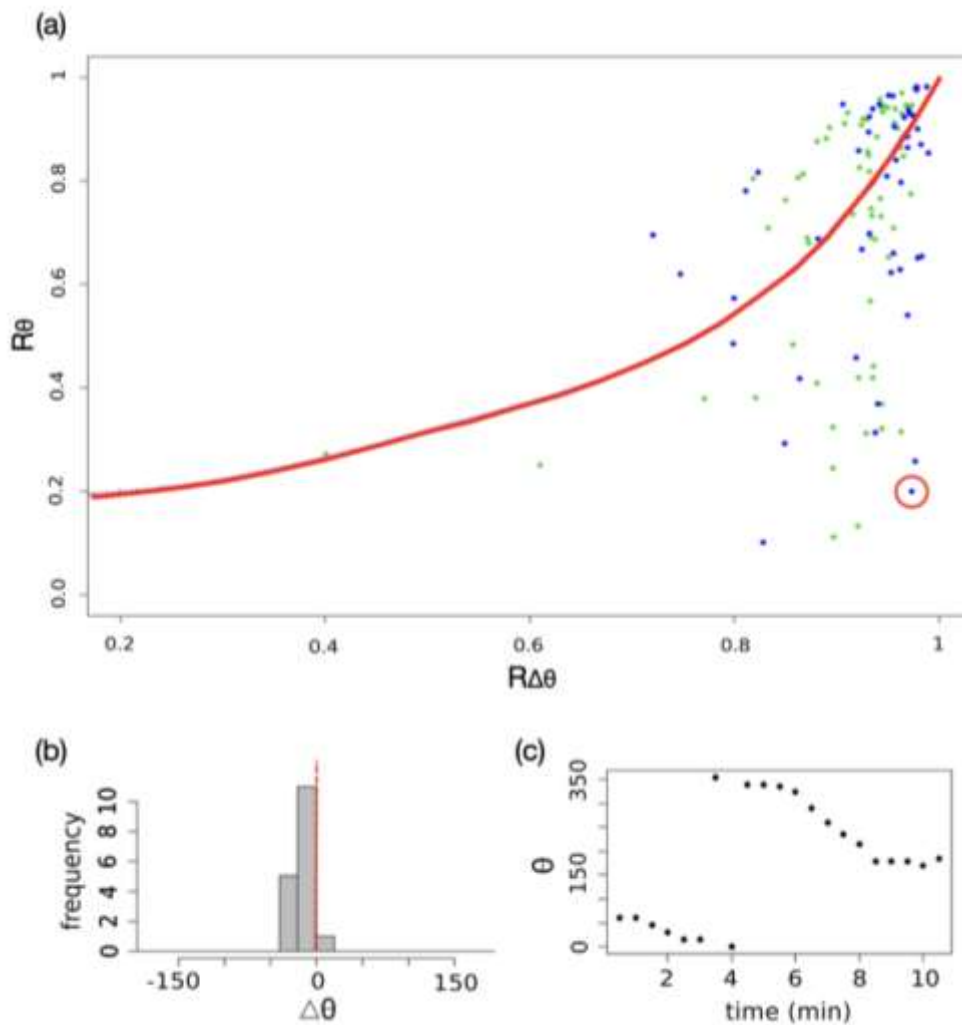
112 **Supplementary Note 5. Running our analyses on trials that do not exhibit irregular** 113 **behavior.**

114 In this section, we examine if trials with irregular behavior may affect our general results which
115 indicate the use of external cues by fish larvae. To achieve this, we visually inspected the
116 movement patterns of *scuba-following* and subsampled *DISC* trials (Nobs=21), and ran our

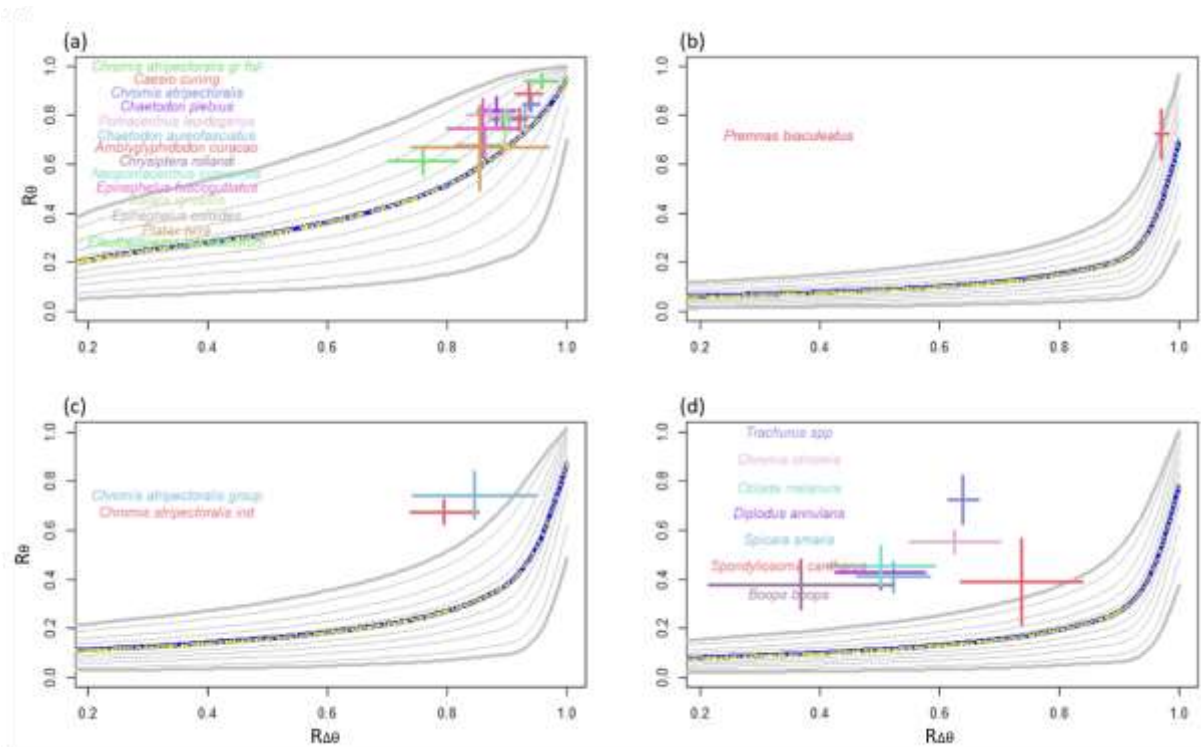
117 analyses on trials that do not seem, based on visual inspection, to demonstrate irregular behavior
118 (i.e., one-sided bias, multi-modal distribution of θ , bi-modal distribution of $\Delta\theta$, composite
119 movement pattern) (Fig. S5). An example of the plots used for the visual inspection are given in
120 Figure S6 for a trial that does not demonstrate irregular behaviors, and in Figure S7 for a trial
121 that demonstrates irregular behavior. This Supplementary note indicated that trials that may
122 contain irregular behaviors do not affect the overall results and conclusion. It is important to note
123 that it is difficult to differentiate between the possible types of irregular behaviors. Some trials
124 represent a combination of a few types (e.g., one-sided drift and composite pattern), and it is also
125 possible that there are other types of irregular behaviors that are not considered. In addition, it is
126 possible that despite the irregular behaviors the trial would be correctly categorized, meaning
127 that a larva that was actually using extremal cues for orientation would have been correctly
128 categorized as such, and vice-versa.

129 **Supplementary References**

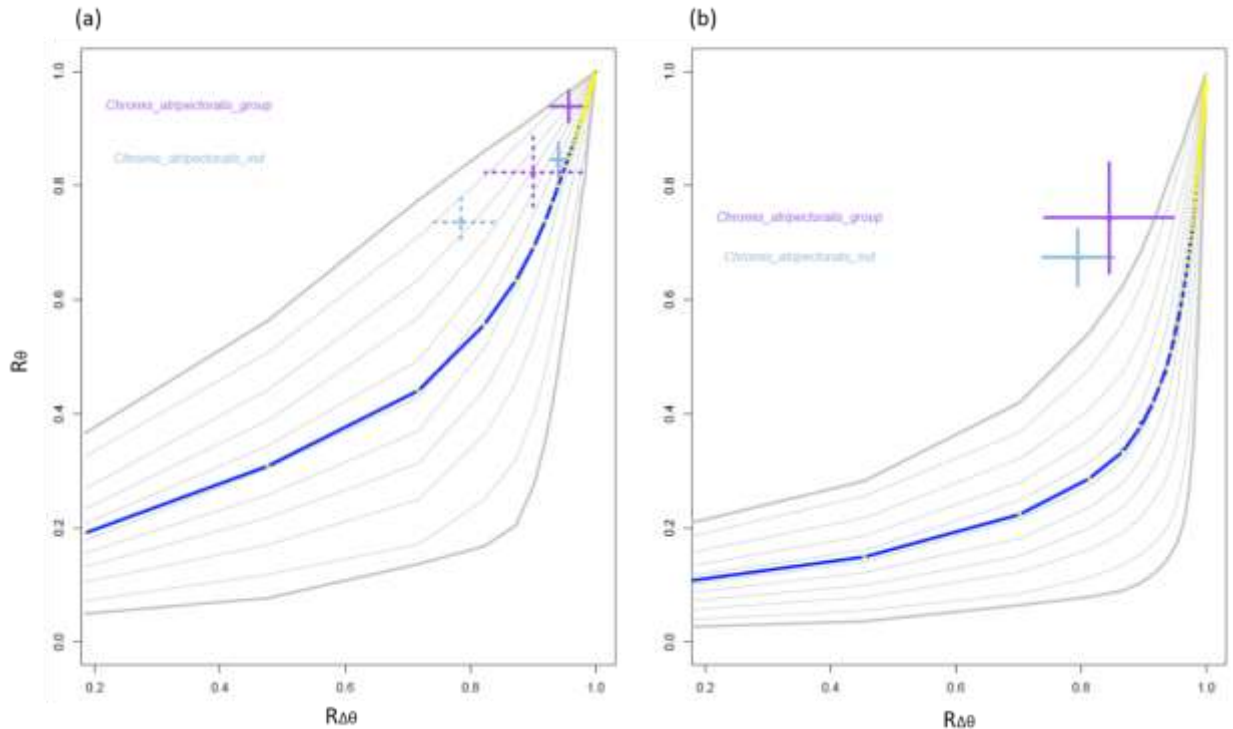
- 130 1. Leis, J. M. Vertical distribution behaviour and its spatial variation in late-stage larvae of
131 coral-reef fishes during the day. *Mar. Freshw. Behav. Physiol.* **37**, 65–88 (2004).
- 132 2. Leis, J. M. & Carson-Ewart, B. M. Orientation of pelagic larvae of coral-reef fishes in the
133 ocean. *Mar. Ecol. Prog. Ser.* **252**, 239–253 (2003).
- 134 3. Leis, J. M., Wright, K. J. & Johnson, R. N. Behaviour that influences dispersal and
135 connectivity in the small, young larvae of a reef fish. *Mar. Biol.* **153**, 103–117 (2007).
- 136 4. Bailey, J. D. & Codling, E. A. Emergence of the wrapped Cauchy distribution in mixed
137 directional data. *AStA Adv. Stat. Anal.* 1–18 (2020).
- 138 5. Irisson, J.-O., Paris, C. B., Leis, J. M. & Yerman, M. N. With a little help from my
139 friends: group orientation by larvae of a coral reef fish. *PLoS One* **10**, e0144060 (2015).
- 140 6. Leis, J. M., Paris, C. B., Irisson, J.-O., Yerman, M. N. & Siebeck, U. E. Orientation of fish
141 larvae in situ is consistent among locations, years and methods, but varies with time of
142 day. *Mar. Ecol. Prog. Ser.* **505**, 193–208 (2014).



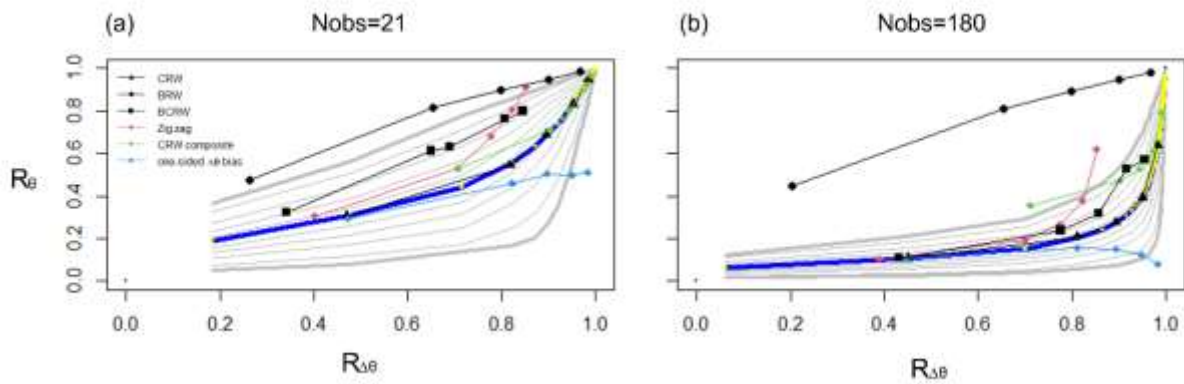
143 **Figure S1. Example of Correlated Random Walk von Mises (CRW-vm) analysis of**
 144 **individual larvae of the species *Chaetodon aureofasciatus* and *Amblyglyphidodon curacao*.**
 145 (a) $(\hat{R}_{\Delta\theta}, \hat{R}_{\theta})$ of *C. aureofasciatus* (blue) and *A. curacao* (green). Circled in red is an orientation
 146 trial of an individual *C. aureofasciatus* which did not exhibit a straighter movement (i.e., higher
 147 mean vector length) than expected under CRW (i.e., $\hat{R}_{\theta} < \bar{R}_{\theta_0^{vm}}$). Red line in (a) represents the
 148 mean CRW-vm (Figure 2). (b) *Turning angles* distribution ($\Delta\theta$), and (c) *bearings* (θ) versus trial
 149 time of the *C. aureofasciatus* larva marked in red in (a).
 150
 151



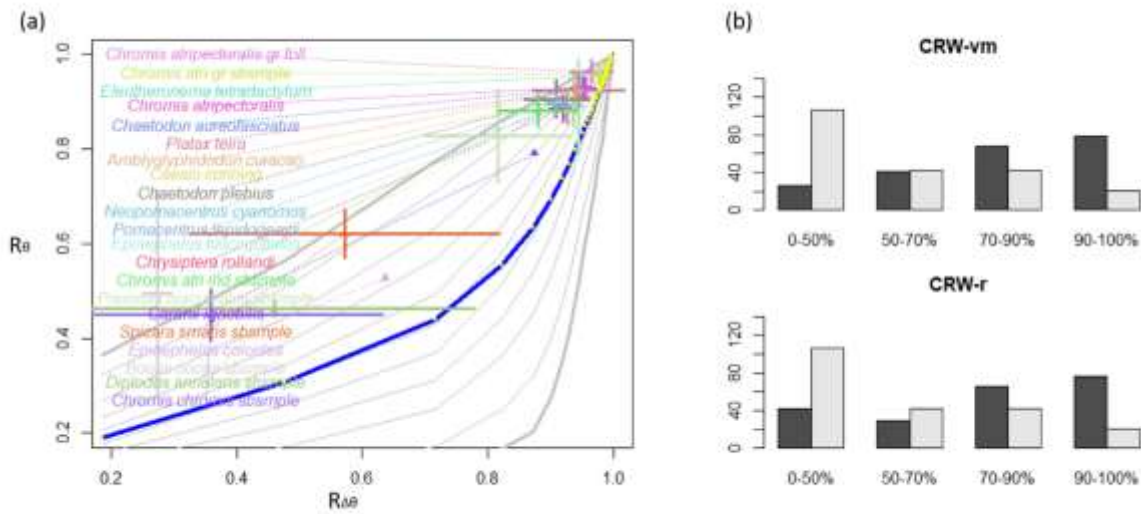
152 **Figure S2. Correlated Random Walk wrapped Cauchy (CRW-wc) analysis at the species**
 153 **level.** The analysis is based on the diagram in (Figure 2c) with the wrapped Cauchy distribution
 154 replacing the von Mises distribution. Panels represent the scuba-following trials (a), and for the
 155 *DISC* trials (b-d) with various number of samples-per-trial: $N_{obs}=21$ (a), 300 (B), 90 (c), and 180
 156 (d). Crosses represent means \pm 95% Confidence Interval (CI) of the observed $(\hat{R}_{\Delta\theta}, \hat{R}_{\theta})$ pooled
 157 by species. Thick blue line represents the curve fitted through the means of $(R_{\Delta\theta}^{wc}, R_{\theta}^{wc})$,
 158 generated for each ρ value (yellow dots on top of the curve). Species names are ordered top-
 159 down according to their \hat{R}_{θ} means and correspond in color to their respective crosses.



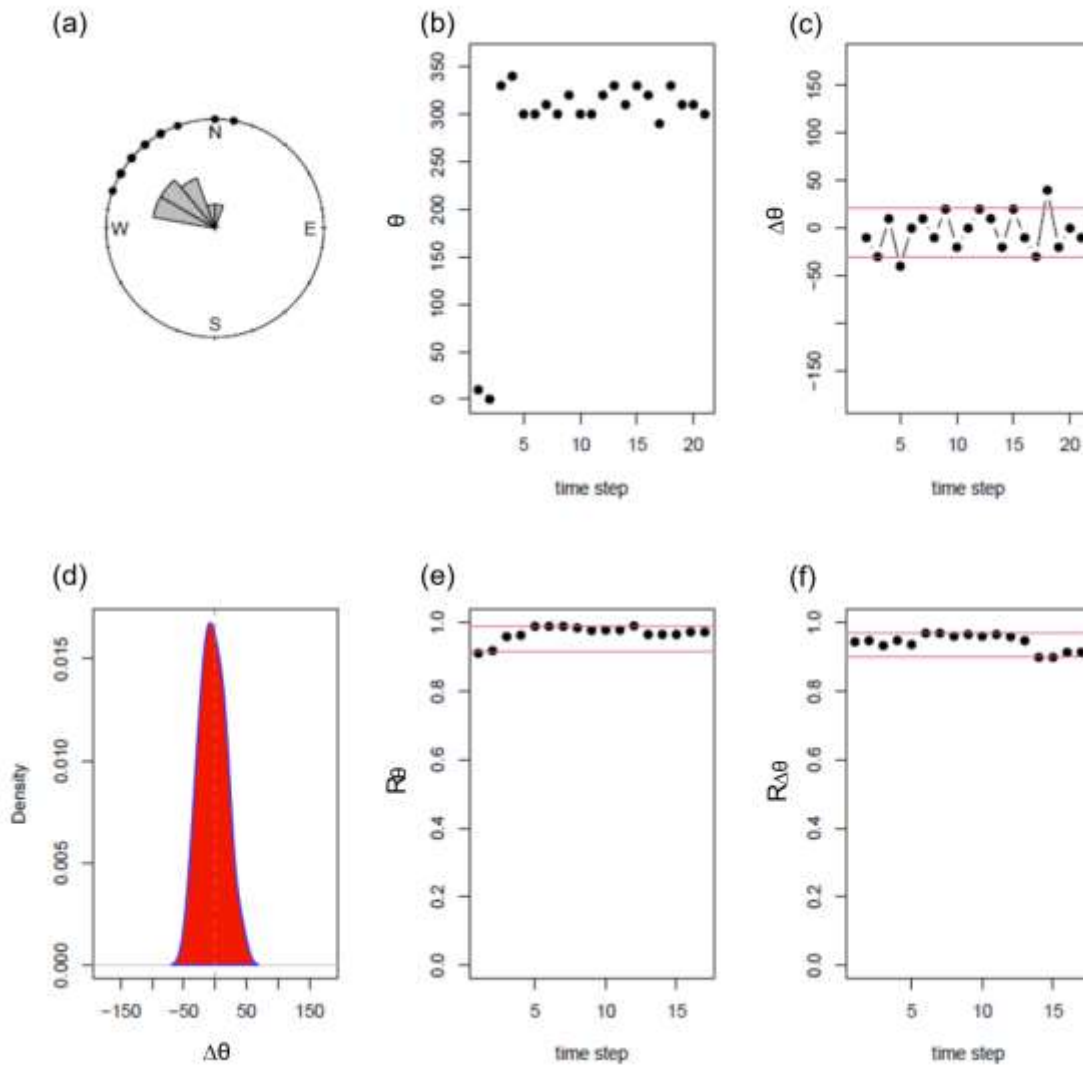
160
 161 **Figure S3. Comparison between scuba-following (a) and DISC (b) trials of individuals**
 162 **(cyan) and groups (magenta) of *Chromis atripectoralis* settlement-stage larvae using**
 163 **Correlated Random Walk von Mises (CRW-vm).** Dotted crosses represent the trials in (b)
 164 which were sub-sampled to contain 21 observations (N_{obs}) per trial. The analysis is based on the
 165 diagram in (Figure 2c). Crosses represent means \pm 95% Confidence Interval (CI) of the observed
 166 $(\hat{R}_{\Delta\theta}, \hat{R}_\theta)$.



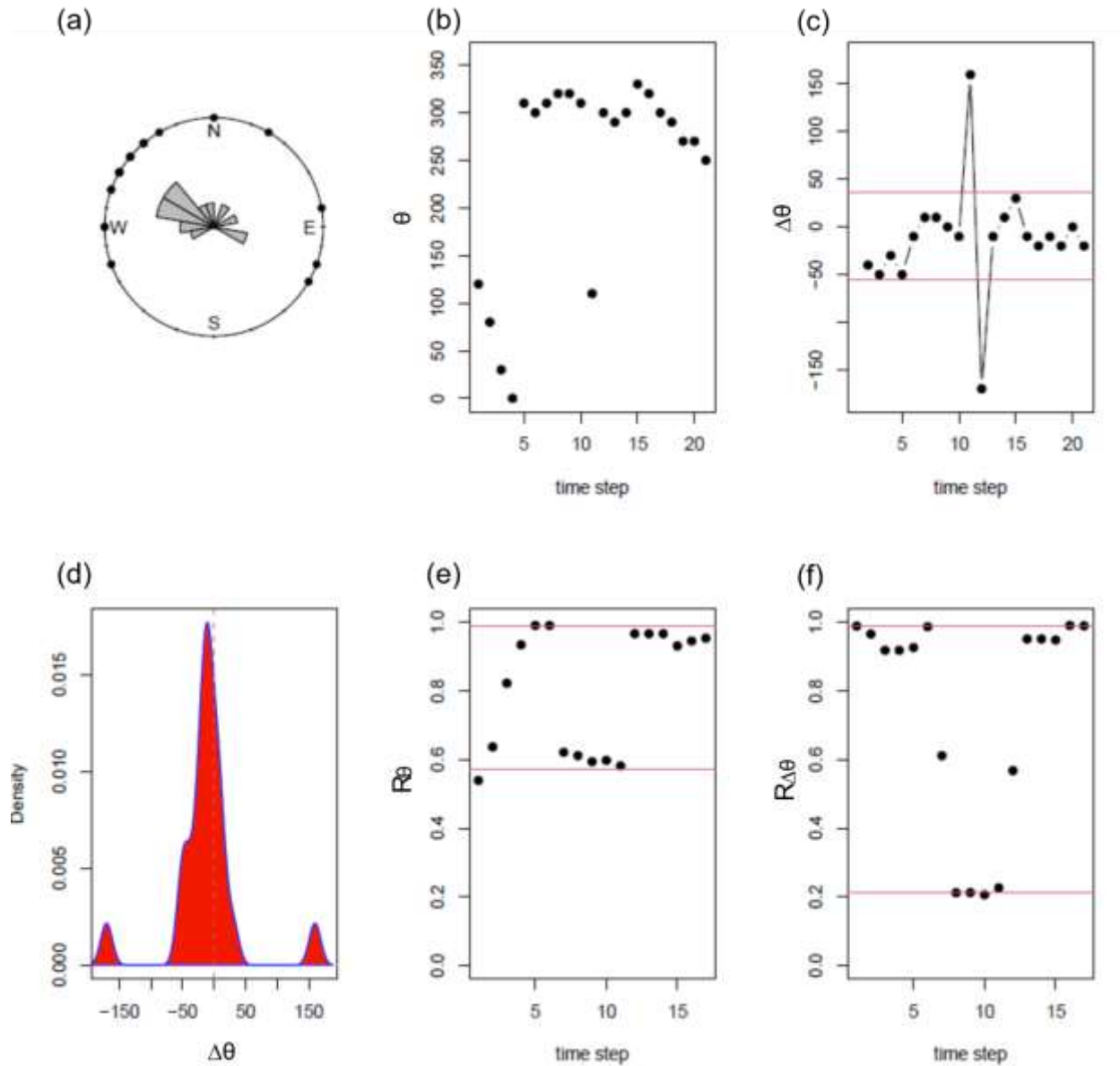
167
 168 **Figure S4. Simulated examples of classic and irregular patterns.** Simulated classic patterns
 169 include Correlated Random Walk (CRW), Biased Random Walk (BRW), and Biased Correlated
 170 Random Walk (BCRW); irregular patterns include bimodal distribution on turning angles ($\Delta\theta$;
 171 zig zag), movement pattern in which $kappa$ parameter of $\Delta\theta$ distribution changes halfway
 172 through the simulation (CRW composite), and one-sided $\Delta\theta$ bias. Movement patterns are
 173 simulated for $kappa=1, 3, 5, 10, 30$ and number of observations of (a) Nobs=21 and (b)
 174 Nobs=180. More details about these simulations and their parametrization are given in Table
 175 S1.



176 **Figure S5. Correlated Random Walk-von Mises (CRW-vm) and Correlated Random Walk**
 177 **resampling (CRW-r) results for trials that do not demonstrate irregular behavior.** This
 178 analysis was performed on trials with Nobs=21, i.e., on *scuba-following* and subsampled *DISC*
 179 trials that do not seem to demonstrate irregular behavior, i.e., one-sided bias, multi-modal
 180 distribution of bearings (θ), bi-modal distribution of turning angles ($\Delta\theta$), and *CRW* composite
 181 movement pattern (N=214,). Legend details are the same as in Fig. 1. Examples of trials without
 182 and with irregular patterns are given in supplementary Figs. S6 and S7, respectively. Triangles
 183 represent species that included a single individual in this analysis.
 184
 185
 186



187
 188 **Figure S6. Visual inspection for detecting irregular behaviors- an example that does not**
 189 **show irregular patterns.** An example a trial (*Caesio cuning, scuba-following*) that does not
 190 show irregular patterns of: one-sided bias, multi-modal distribution of bearings (θ), bi-modal
 191 distribution of turning angles ($\Delta\theta$), or composite movement pattern. The panels show: (a) rose
 192 diagram of θ , (b) θ over time, (3) $\Delta\theta$ over time, (4) $\Delta\theta$ density distribution, (5) moving window
 193 of \hat{R}_θ (window's length =4 steps), (6) moving window of $\hat{R}_{\Delta\theta}$ (window's length =4 steps).
 194 Horizontal red lines represent the inter-percentile range (5-95%).



195 **Figure S7. Visual inspection for detecting irregular behaviors- an example that shows**
 196 **irregular patterns.** An example of a trial (*Chaetodon aureofasciatus*, scuba-following) that
 197 shows several irregular patterns: (1) one-sided bias towards left turns, multi-modal distribution
 198 of bearings (θ) (top left panel), and composite movement pattern in which movement precision is
 199 not homogenous and changes substantially between different stages of the trial. The panels show:
 200 (a) rose diagram of θ , (b) θ over time, (3) turning angles ($\Delta\theta$) over time, (4) $\Delta\theta$ density
 201 distribution, (5) moving window of \hat{R}_θ (window's length =4 steps), (6) moving window of $\hat{R}_{\Delta\theta}$
 202 (window's length =4 steps). Horizontal red lines represent the inter-percentile range (5-95%).

Table S1 Simulation details for simulated examples of classic and irregular patterns (Supplementary note 4). Common parameters for all simulations include $\kappa_{CRW}=1, 3, 5, 10, 30$, number of replicates=1000, number of observations Nobs=21 and 180 for Fig. S4a and S4b, respectively.

Scenario name	Description
CRW	Correlated Random Walk with turning angles drawn from a von Mises distribution centered around zero and κ_{CRW} values of 1, 3, 5, 10, 30
BRW	Biased Random Walk with bearings drawn from a von Mises distribution centered around zero and κ_{BRW} values of 1, 3, 5, 10, 30
BCRW	Biased Correlated Random Walk with turning angles drawn from a von Mises distribution centered around zero and κ_{CRW} values of 1, 3, 5, 10, 30. and re-orientation towards the fixed direction. Re-orientation occurs 0° every 3 and 22 steps for Nobs=21 and 180, respectively, and includes drawing a heading from a von Mises distribution centered around zero with $\kappa_{BRW}=3$, and adding an error term in form of a turning angle drawn from the CRW von Mises distribution above.
Zig zag	Correlated Random Walk with turning angles drawn from two von Mises distributions centered around positive (30°) and negative (-30°) directions and κ_{CRW} values of 1, 3, 5, 10, 30.
CRW composite	A sequence that is composed of two types of CRW patterns, alternating half-way through the sequence (i.e., after Nobs/2 steps). The first type includes turning angles drawn from a von Mises distribution with κ_{CRW} values of 1, 3, 5, 10, 30 and the second type includes factoring the κ_{CRW} by 20, i.e., values of 20, 60, 100, 200, 600. Turning angles distributions of both types are centered around zero.
One-sided $\Delta\theta$ bias	Correlated Random Walk with turning angles drawn from a von Mises distribution centered around 10° and κ_{CRW} values of 1, 3, 5, 10, 30